



Science Arts & Métiers (SAM)

is an open access repository that collects the work of Arts et Métiers Institute of Technology researchers and makes it freely available over the web where possible.

This is an author-deposited version published in: <https://sam.ensam.eu>
Handle ID: <http://hdl.handle.net/10985/25746>



This document is available under CC BY license

To cite this version :

Khayel CHAABANI, Mariem BEN SAADA, BRUNO LAVISSE, Mathieu RITOU, Guenael GERMAIN - Estimation of the residual stress field of laminated aeronautical parts to prevent distortion after machining - In: ESAFORM, France, 2024-04-24 - Materials Research Proceedings - 2024

Any correspondence concerning this service should be sent to the repository

Administrator : scienceouverte@ensam.eu



Estimation of the residual stress field of laminated aeronautical parts to prevent distortion after machining

CHAABANI Khayel^{1,2,3,a*}, BEN SAADA Mariem^{1,b}, LAVISSE Bruno^{1,c},
RITOU Mathieu^{2,d} and GERMAIN Guénaël^{1,e}

¹LAMPA, Arts et Métiers, Angers, France

²LS2N, Nantes Université, Nantes, France

³IRT Jules Verne, Nantes, France

^akhayel.chaabani@ensam.eu, ^bmariem.bensaada@ensam.eu, ^cbruno.lavisse@ensam.eu,

^dmathieu.ritou@univ-nantes.fr, ^eguenael.germain@ensam.eu

Keywords: Distortion, Residual Stresses (RS), Distortion Control, Simulation, Machining

Abstract. The estimation of post-machining distortion of monolithic aeronautical parts induced by the redistribution of the bulk residual stresses (RS) during machining is one of the major challenges of aeronautical parts manufacturing. Since it is the main cause of thick parts post-machining distortion, it is essential to know the state of the initial RS so that the machining strategy can be modified to minimize distortion of each part. The problem is even more complex because the RS field is not identical from one part to another. Considering an average stress field provides satisfactory results only for parts with simple geometries and a highly repeatable manufacturing process, which is rarely the case in an industrial setting. By simulating the steps of the production of the laminated blank, the variability of RS field will be established. This variability can be used to determine the distribution of the RS field of each part during machining.

Introduction

Several industrial sectors, including the automotive, medical, and aerospace industries, heavily rely on aluminum alloy material due to its high strength and corrosion resistance [1, 2]. Aeronautical industries extensively use aluminum laminated blanks which are usually machined in thick plates. To reach high mechanical properties, these blanks are subject to heat treatments (i.e. quenching, tempering, etc.). Thus, they undergo plastic deformations and thermal gradients, during the forming process, due to thermo-mechanical loads which generate in the blanks high intensity residual stresses called also initial Residual Stresses (RS) [3, 4].

For manufacturers, reducing part distortions remains a major challenge even with the widespread use of this material. During forming steps, blank rolled plates undergo heat treatments and plastic deformations which generate RS in the blank.

The blanks are then subject to a machining process aiming to obtain the desired final part shape. The loading applied during this process can also induce RS on the part surface called near-surface RS [4, 5]. Compared to the initial RS, the near-surface RS can be neglected when working with large thick aluminum alloy parts since the affected depth does not exceed a few hundred microns from the top surface [6]. In industry, the main issue is not directly related to the near-surface RS but rather to the distortion of the finished part [1, 7]. The redistribution of the initial RS owing to material removal during machining is the main cause of post-machining distortions (after unclamping). These distortions may cause the parts to be rejected or require additional conforming operations, which could increase the cost of production [1, 2]. Since it is the main cause of thick parts post-machining distortion, it is essential to know the state of the initial RS so that the machining strategy can be modified to minimize distortion of each part.

The RS profiles can be experimentally determined using destructive and non-destructive tests [4, 8, 9]. Among these techniques, the most generally used are the X-ray diffraction, which is more suitable for the surface; and the layer removal or by incremental drilling. The experimental RS profiles are then used to develop Finite Element Models (FEM) which allows simulating machining process and then to predict the machining distortion considering the redistribution of the initial RS [10]. Numerical simulations have been widely used to simulate the RS field in aeronautical parts, as experimental studies are often costly and time-consuming, and may require sacrificing the part to carry out the measurements [11, 12].

The approach of the present work aims to establish a hybrid methodology to predict the variability of the RS field induced in aluminum bulk blanks, due to the manufacturing history of the blank. This enables controlling the machining strategy at each stage to reduce the final part distortions. This approach is detailed in the section “Proposed methodology” and then the results of the variability of the initial RS field are presented. This present paper focuses only on the first part of the proposed approach which is the numerical simulations of the variability of the initial RS field.

Proposed methodology

Part distortion is caused by the release and redistribution of the RS generated by forming and heat treatments applied before machining. Improving initial RS field comprehension allows the definition of a more effective machining strategy to reduce post-machining distortions. For this purpose, we have implemented this methodology, wherein the preparation stage of this approach consists of simulating the manufacturing process of the bulk of laminated blanks using Finite Element Method (FEM). Numerical simulations under the same experimental conditions were performed using Abaqus software. These simulations enable therefore to determine the variability of the initial RS field induced by process variability. This part of the work will be carried out only once since the applied manufacturing process that is being used is unchanged. Once quantified, the initial RS will be used later in an Artificial Intelligence (AI) model. This AI model will be applied to predict the RS field for each bulk blank. The estimated RS field will allow us to control the machining strategy at all its stages in order to reduce the part distortions. After each machining step, in-process distortion measurements will be taken and integrated in the developed machining model to adjust the next machining step.

Concerning the blank manufacturing process, before quenching, the plates undergo a solution heat treatment (a homogenization thermal cycle), as shown in Fig.1, in order to relieve the RS induced by the plastic deformations during the rolling steps. It is assumed that the RS field is free after the solution heat treatment.

During quenching process, thick aluminum blanks of 7010 alloys were submerged in a uniform heat treatment solution which is supposed to remove the RS induced by lamination. The parts are maintained at 470 °C for many hours and then, they are subject to a sudden immersion in the water at 20 °C which is a common quenching media for Al alloys. In this model, the material's behavior is governed by a modified power law. The mechanical properties of the Al7010-T7451 are thermo-dependent and all parameters are confidential properties.

After quenching, the temperature distribution is inserted in a static analysis to release the RS.

A cold stretch or a detensioning by traction is then carried out in the range of 1,5% to 3% before releasing the stresses at the last step.

We did not simulate tempering step due to huge simulation time of the coupled thermomechanical simulation. The influence of the tempering stage on the RS field is very slight, as the temperature rise is slow and fairly low, resulting no significant thermal gradient. There is therefore no stress gradient due to expansion in this manufacturing stage. Thus, this stage has not been simulated.

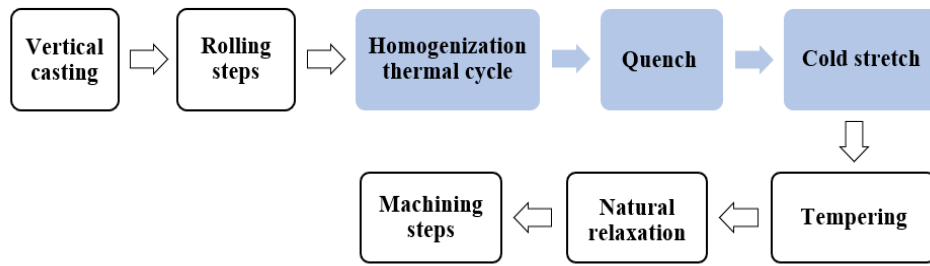


Fig. 1 Forming and heat treatment process

Simulation setting

The final use case concerns large parts of aeronautic structure that are machined in long and thick laminated blank of Al7010 or Al7050 Aluminum. The alloy Al7010 which is of European origin has properties similar to the American Grade 7050. For example, the blank can measure approximately 3 m long, 1 m width, and 120 mm thickness. To carry out a simulation of a three meters length part, the calculation time is oversized. Assuming an isotropic behavior of the material, we have opted for a more effective model. The simulated part measures 800 mm long, 800mm width and 120mm thickness and we have considered the symmetric property of the part. These dimensions are more than sufficient to avoid edge effect. The results shown in Fig. 2 (a) clearly demonstrate the edge effect and that the stress field becomes stable at the center of the part. This observation shows that the dimensions chosen for the model mean that it is not affected by edge effects. A total of 76800 5mm-sized hexahedral components were used to mesh the plate. The mesh type is “DC3D8” during heat transfer step and “C3D8R” during static ones.

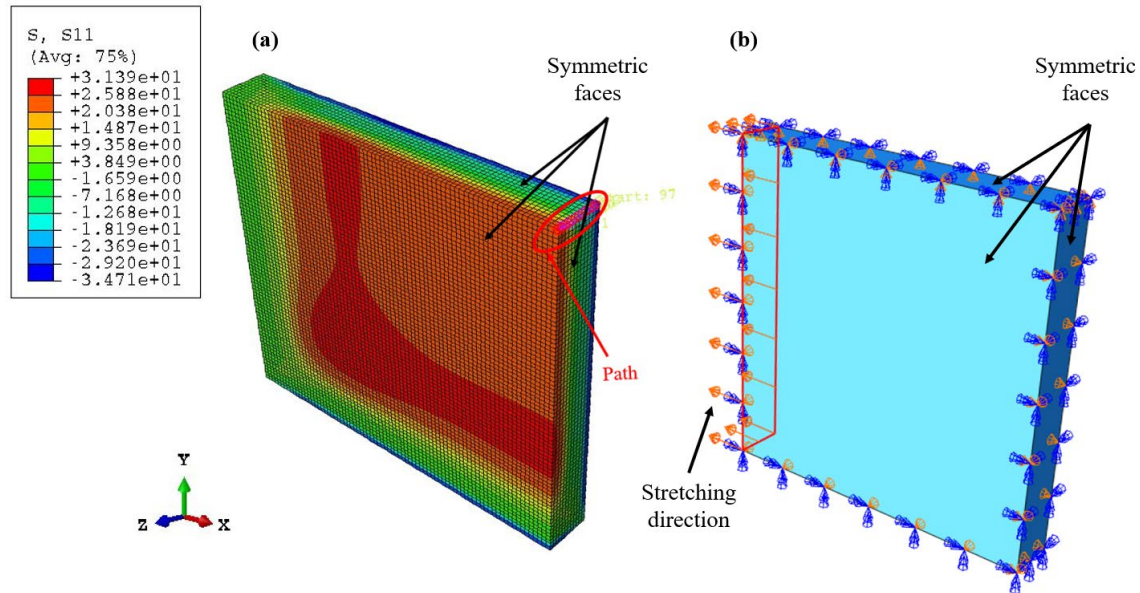


Fig. 2 (a) RS field (S11) after quenching and cold stretching stages with the nominal parameters – (b) Boundary conditions

For the quenching step, heat transfer is modeled by assigning an initial temperature of 470°C to the part. During cooling, the external surfaces of the part are subject to a convection-type boundary condition, with an exchange coefficient h depending on the part temperature and a constant bath temperature (see Table 1). The other surfaces have symmetrical boundary conditions, implying no heat exchange on these surfaces. For the cold stretching step, the symmetry conditions are maintained (Fig. 2b). On the end surface, a homogeneous displacement was imposed to obtain

the desired elongation (see Table 1). Figure 2a shows an example of the RS field obtained after stretching.

To simulate the effect of the heat treatments, it is conventional to separate the thermal simulation from the mechanical simulation, in order to limit the resources required and save calculation time [4, 13].

In this approach, the thermomechanical problem is assumed to be uncoupled: the thermal and mechanical analysis are solved sequentially and consecutively. This assumption allows controlling complex phenomena released during the heat treatment process, that leads to a better representation of the RS distribution. The simulation steps can be summarized in four principal tasks as shown in Fig. 3: initially, a non-linear heat transfer analysis is carried out, considering the thermo-dependent mechanical parameters. Subsequently, a thermo-elastoplastic analysis using the predicted temperature distributions, assuming an isotropic behavior of the material and considering the temperature dependence of its mechanical properties.

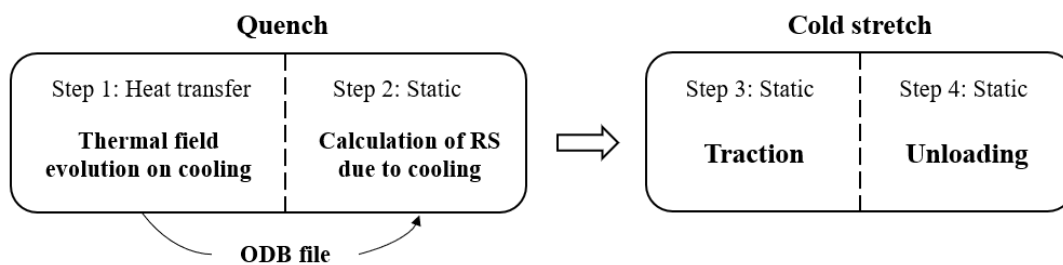


Fig. 3 Steps followed in the numerical simulation model

The variability of the manufacturing process parameters is the main cause of the initial RS field's variability. Three parameters are studied during these simulations as shown in the Table 1:

- The temperature of the quench bath: 20°C is the nominal temperature of the quench.
- The thermal convection coefficient with water *h*: several parameters affect the thermal convection coefficient like the temperature of the water, its flow, etc. The thermal convection coefficient used during these simulations is temperature dependent and taken from the literature [14]. “*h*” referred in Table 1 is the nominal one of the simulations.
- The cold stretch or elongation range: in general, the plate is stretched by classical traction between 1.5 and 3%.

In order to represent this variability, we carried out several numerical simulations combining the different parameters. The results of these simulations will be discussed in the next section.

Table 1. Simulation plan of the process parameters variability

Process parameters	Variability				
Bath temperature	18°C	20°C	25°C	30°C	----
Thermal convection coefficient	<i>h</i>	1.5 * <i>h</i>	2 * <i>h</i>	2.5 * <i>h</i>	3 * <i>h</i>
Cold stretch rate	1.5%	2%	2.5%	3%	3.5%

Results and discussion

During quenching, the cooling rate is not uniform from the surface to the core of the part, creating a thermal gradient. The contraction of the part's core during cooling will therefore compress the part's surface, as shown in Fig. 4. The RS fields depicted in Figures 4 to 8 correspond to the values along the path illustrated in Fig. 2 (a).

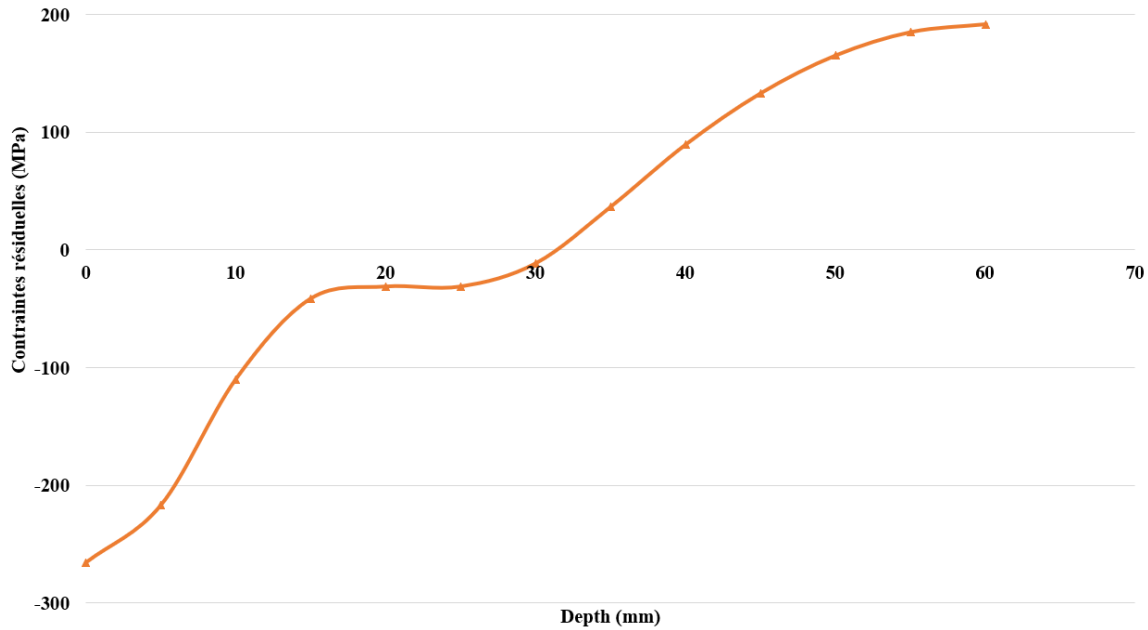


Fig. 4 Shape of half of the RS field along the half of the thickness of the rolled plate

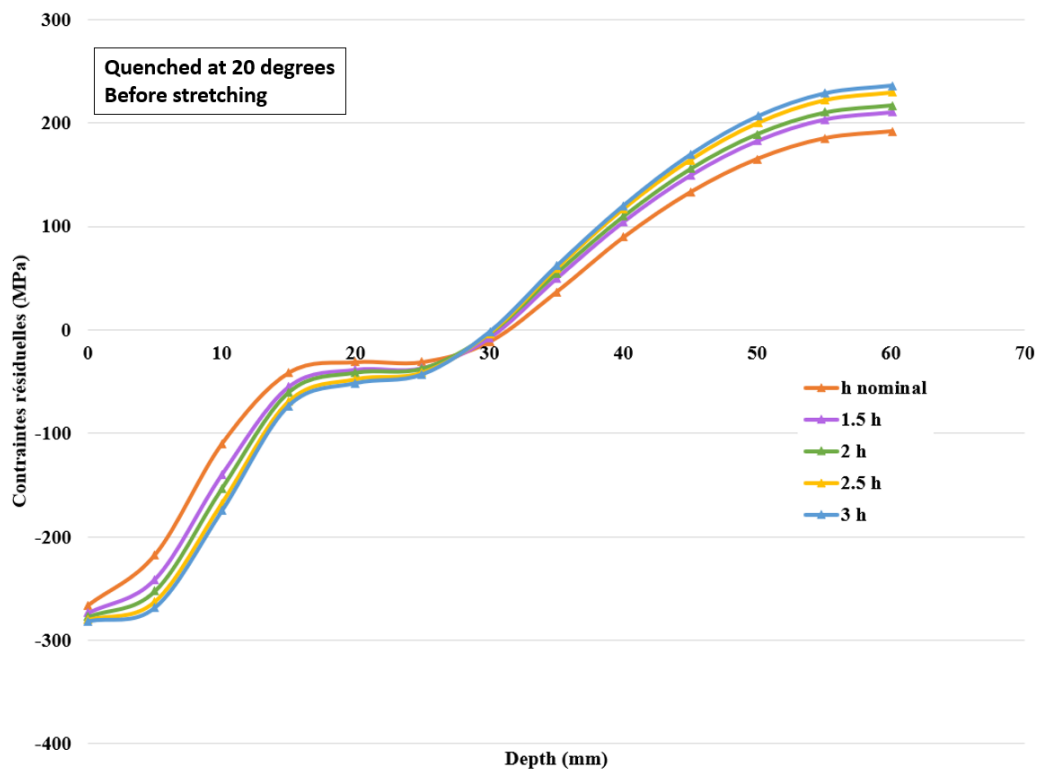


Fig. 5 Thermal convection coefficient's influence on the RS field

The variability of the thermal convection coefficient has a significant impact on RS, as it depends on various factors such as the quenching bath temperature, water flow rate, whether convection is forced or natural, etc. This variability affects both the surface and the core of the part, as shown in Fig. 5.

The quench bath temperature has little impact on the core of the part, resulting in an increase in compression of a few MPa as the bath temperature decreases, from 192 MPa at 18 degrees to 184 MPa at 30 degrees. This influence remains limited to the core of the part and does not significantly affect the stresses at the surface as shown in Fig. 6.

During cold stretch, the elongation value has a significant influence on the distribution of the stress field as shown in Fig. 8. Indeed, stretching results in a significant reduction of core stresses, decreasing from 191 MPa before stretching to 20 MPa after a 3% stretch, as illustrated in Fig. 8. Similarly, at the surface, compression stresses increase from -265 MPa before stretching to -31 MPa after a 3% stretch. Stress values and gradients after stretching are therefore lower, which will greatly limit part deformation after machining. Thus, a well-controlled elongation value ensures a predictable and consistent stress distribution within the material. This underscores the need for meticulous control to minimize undesired stress field variations. A variation in elongation from 1.5% to 3.5%, as shown in Fig. 7, causes the surface stress to vary from approximately -120 MPa to -20 MPa, an impressive reduction of 100 MPa.

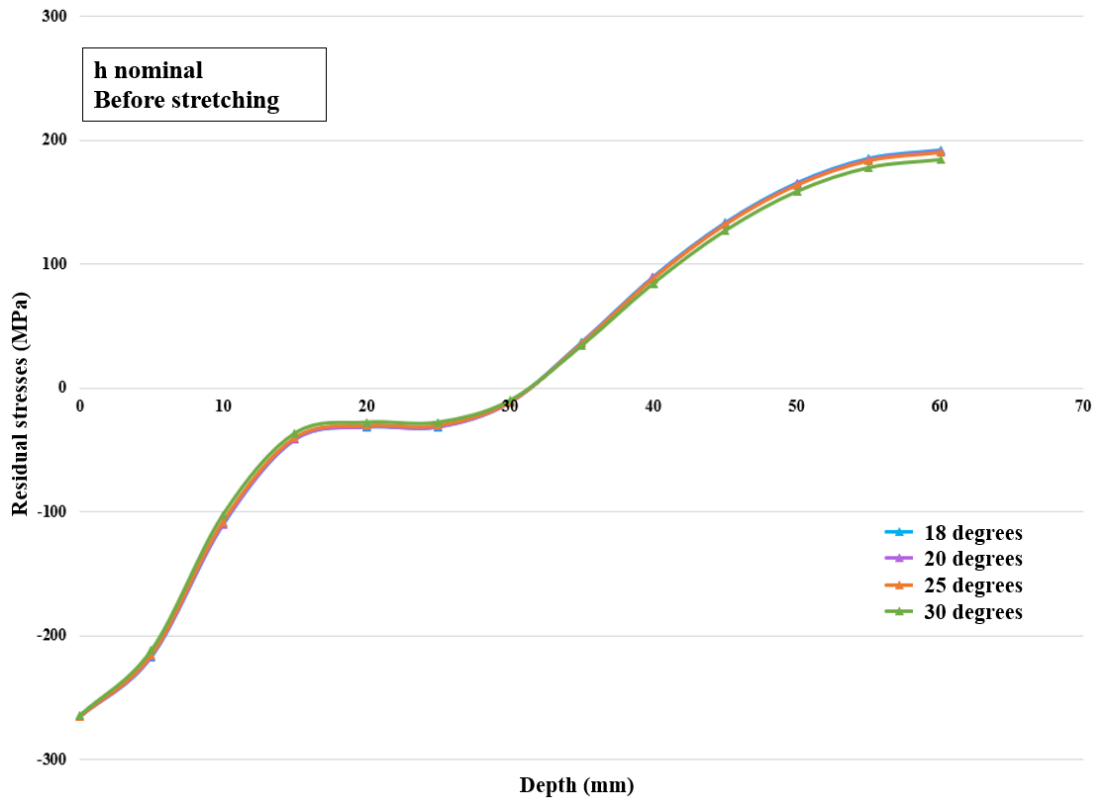


Fig. 6 Quenching bath temperature's influence on the RS field

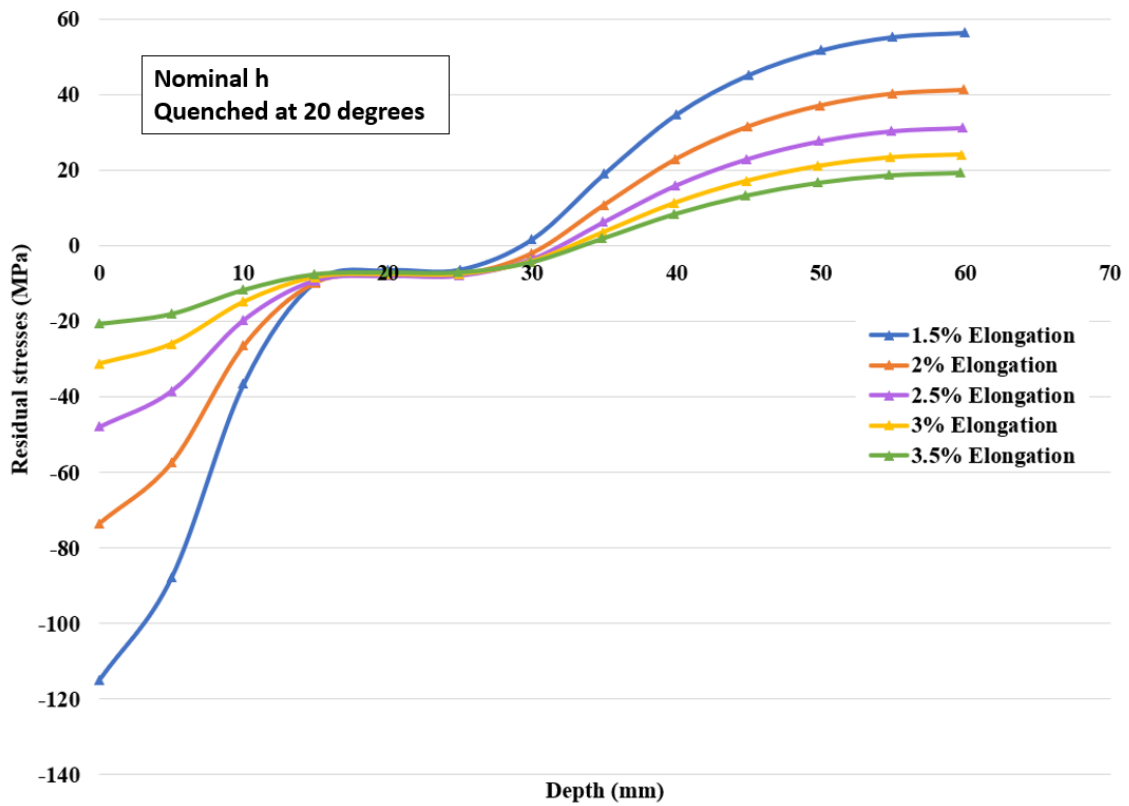


Fig. 7 Effect of the elongation value on the RS field

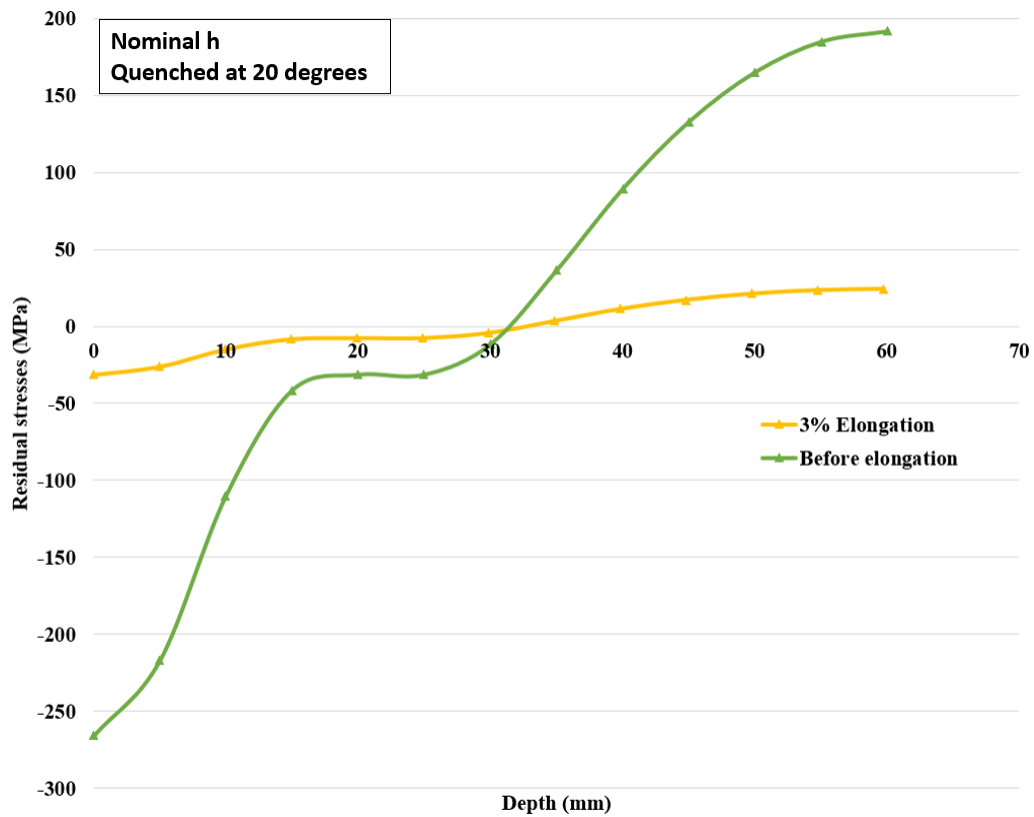


Fig. 8 RS field before and after elongation

Sensitivity study

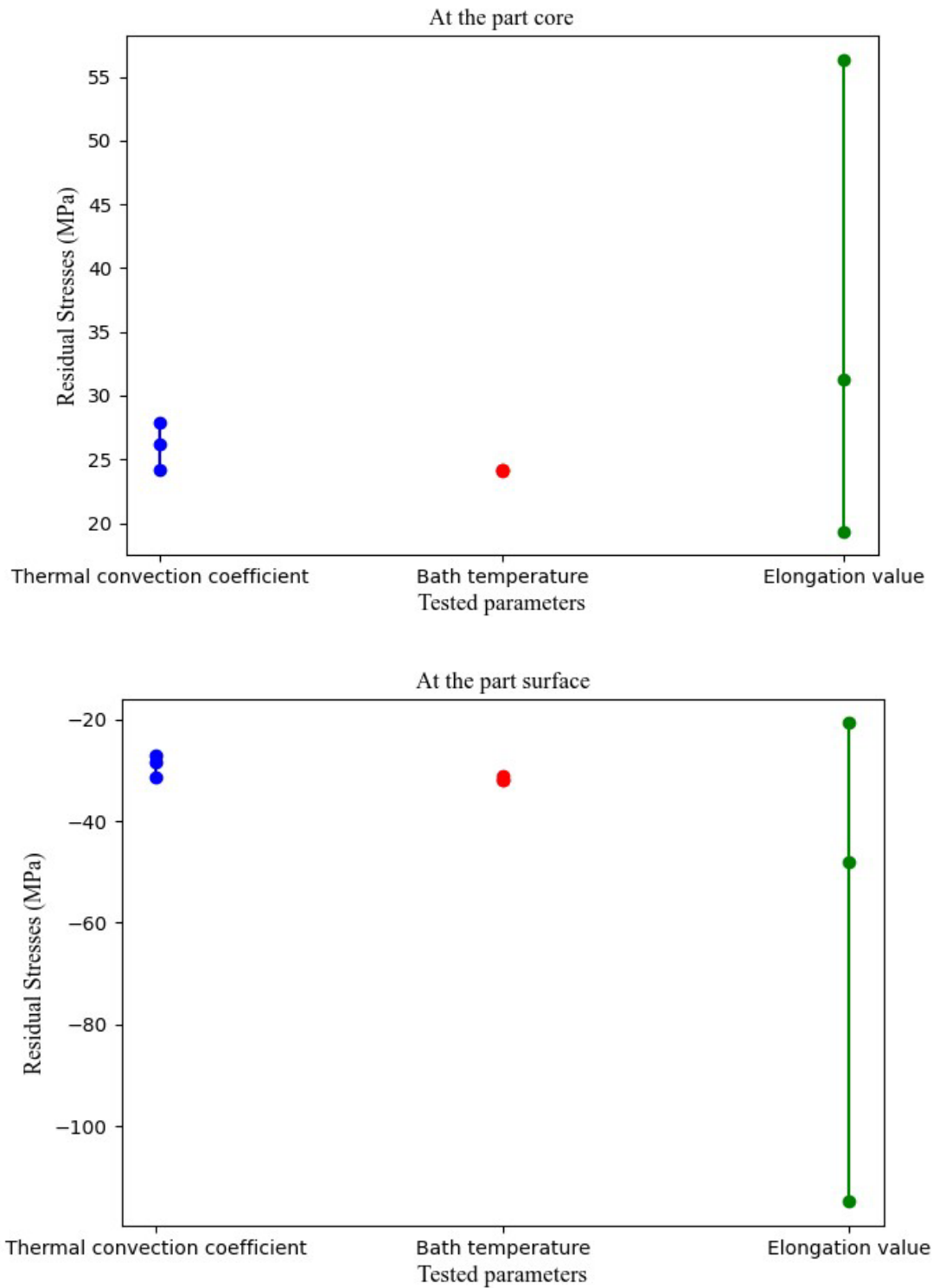


Fig. 9 Parameters sensitivity analysis results

Based on this finite element model, we assessed the sensitivity of RS to process parameters during the forming and heat treatment of the blank parts. The parameters sensitivity analysis is illustrated in Fig. 9.

This analysis reveals that the initial stress field of the part, encompassing both surface and core, is exclusively influenced by the applied elongation value during the stretching step, and the thermal convection coefficient of the quenching medium.

Depending on the deformation of the part obtained at the start of machining, it will be possible to estimate the elongation value and the thermal convection value applied to the part and thus know the stress field of the part during manufacture (with the future IA model). In this way, it will be possible to modify the strategy at the end of the machining stage to minimize the final deformation of the part.

Conclusions

In this work, a thermomechanical model was developed to simulate the manufacturing process of aluminum alloy laminated blanks on Abaqus software. Several numerical simulations, combining the different material parameters, have been carried out to determine the initial RS field's variability.

The results show that the variability of quenching temperature does not significantly influence the final stress field. On the other hand, the stretching step plays a crucial role in stress distribution. The thermal convection coefficient also influences the stress field, but to a much lesser extent. This highlights the need for meticulous control for these parameters to reduce undesirable stress variations.

Based on these results, variations in the RS field are now known as a function of operating parameters. This will make it possible to predict the distribution of the RS field for each part during machining, offering a proactive approach to prevent distortions.

Acknowledgements

The authors acknowledge the funding of PERFORM Program of IRT Jules Verne.

References

- [1] Sim W-M (2010) Challenges of residual stress and part distortion in the civil airframe industry. *International Journal of Microstructure and Materials Properties* 5:446–455. <https://doi.org/10.1504/IJMMP.2010.037621>
- [2] Li J, Wang S (2017) Distortion caused by residual stresses in machining aeronautical aluminum alloy parts: recent advances. *Int J Adv Manuf Technol* 89:997–1012. <https://doi.org/10.1007/s00170-016-9066-6>
- [3] Tang ZT, Yu T, Xu LQ, Liu ZQ (2013) Machining deformation prediction for frame components considering multifactor coupling effects. *Int J Adv Manuf Technol* 68:187–196. <https://doi.org/10.1007/s00170-012-4718-7>
- [4] Jeanmart P, Bouvaist J (1985) Finite element calculation and measurement of thermal stresses in quenched plates of high-strength 7075 aluminium alloy. *Materials Science and Technology* 1:765–769. <https://doi.org/10.1179/mst.1985.1.10.765>
- [5] Denkena B, De Leon L (2008) Milling induced residual stresses in structural parts out of forged aluminium alloys. *International Journal of Machining and Machinability of Materials* 4:335–344. <https://doi.org/10.1504/IJMMM.2008.023717>
- [6] Chatelain J-F, Lalonde J-F, Tahan AS (2012) Effect of Residual Stresses Embedded within Workpieces on the Distortion of Parts after Machining. 6:
- [7] Lequeu P, Lassince P, Warner T, Raynaud GM (2001) Engineering for the future: weight saving and cost reduction initiatives. *Aircraft Engineering and Aerospace Technology* 73:147–159. <https://doi.org/10.1108/00022660110386663>

- [8] Virkar AV (1990) Determination of Residual Stress Profile Using a Strain Gage Technique. *Journal of the American Ceramic Society* 73:2100–2102. <https://doi.org/10.1111/j.1151-2916.1990.tb05276.x>
- [9] Tandon R, Green DJ (1990) Residual Stress Determination Using Strain Gage Measurements - Tandon - 1990 - *Journal of the American Ceramic Society* - Wiley Online Library. <https://ceramics.onlinelibrary.wiley.com/doi/abs/10.1111/j.1151-2916.1990.tb06738.x>. Accessed 5 Feb 2024
- [10] Wei Y, Wang XW (2007) Computer simulation and experimental study of machining deflection due to original residual stress of aerospace thin-walled parts. *Int J Adv Manuf Technol* 33:260–265. <https://doi.org/10.1007/s00170-006-0470-1>
- [11] Cerutti X, Arsene S, Mocellin K (2015) Prediction of Machining Quality due to the Initial Residual Stress Redistribution of Aerospace Structural Parts Made of Low-Density Aluminium Alloy Rolled Plates. *International Journal of Material Forming* 9:. <https://doi.org/10.1007/s12289-015-1254-7>
- [12] Chabeauti H, Ritou M, Lavisse B, et al (2023) Digital twin of forged part to reduce distortion in machining. *CIRP Annals* 72:77–80. <https://doi.org/10.1016/j.cirp.2023.04.021>
- [13] Lamba NK, Khobragade NW (2012) Uncoupled thermoelastic analysis for a thick cylinder with radiation. *Theoretical and Applied Mechanics Letters* 2:021005. <https://doi.org/10.1063/2.1202105>
- [14] Louhichi MA, Poulachon G, Lorong P, et al (2022) Experimental and simulative determination of residual stress during heat treatment of 7075-T6 aluminum. *Procedia CIRP* 108:82–87. <https://doi.org/10.1016/j.procir.2022.03.018>